NANO LETTERS

XXXX
Vol. xx, No. x
-

Direct Imaging of Lattice Atoms and Topological Defects in Graphene Membranes

Jannik C. Meyer,[†] C. Kisielowski,[‡] R. Erni,[‡] Marta D. Rossell,[‡] M. F. Crommie,[†] and A. Zettl*,[†]

Materials Sciences Division, Lawrence Berkeley National Laboratory and Department of Physics, University of California at Berkeley, and National Center for Electron Microscopy, Lawrence Berkeley National Laboratory, Berkeley, California 94720

Received May 14, 2008

ABSTRACT

We present a transmission electron microscopy investigation of graphene membranes, crystalline foils with a thickness of only 1 atom. By using aberration-correction in combination with a monochromator, 1-Å resolution is achieved at an acceleration voltage of only 80 kV. The low voltage is crucial for the stability of these membranes. As a result, every individual carbon atom in the field of view is detected and resolved. We observe a highly crystalline lattice along with occasional point defects. The formation and annealing of Stone−Wales defects is observed in situ. Multiple five- and seven-membered rings appear exclusively in combinations that avoid dislocations and disclinations, in contrast to previous observations on highly curved (tube- or fullerene-like) graphene surfaces.

Graphene is a single atomic layer of graphite that has only recently become experimentally accessible in an isolated form.[1,2] Because the electronic, thermal, and mechanical properties of graphene are exceptionally sensitive to lattice imperfections,[3–6] a study of defects in this material is critically important. Although highly curved graphene derivatives such as carbon nanotubes and fullerenes have been studied extensively,[9–11] defects and their dynamics in a planar graphene remain experimentally unexplored.

The optimal experimental configuration for defect study in planar graphene would be free-standing membranes, that is, crystalline foils with a thickness of only 1 carbon atom, probed by a microscopy with true single-atom resolution and with a sufficient data acquisition rate to record real-time defect formation and dynamics. Although it would seem that transmission electron microscopes (TEMs) are ideally suited to this task, traditional TEMs lack the necessary resolution at the required low operating voltages. Here we show the first results obtained with a new microscope design, the aberration-corrected, monochromated TEAM 0.5 transmission electron microscope, operated at 80 kV.[7,8] This unique microscope achieves subangstrom resolution even at 80 kV, thus providing the capability to resolve every single carbon atom in the graphene lattice even for suspended single-layer graphene. Indeed, experimentally we find that, even for single-shot data aquisition, each atom in the field of view is detected with a signal well above the noise. We are able to directly image theoretically predicted configurations such as Stone−Wales defects and explore their real-time dynamics. We find that the dynamics are significantly different from those for closed-shell graphenes such as nanotubes or fullerenes.

Graphene membranes were prepared as described in ref 12. In brief, graphene was isolated on a silicon wafer with a 300-nm oxide layer by mechanical cleavage and located by optical microscopy. A commercially available TEM grid (c-flat, Protochips inc.) with 1-μm holes was placed onto the flake and the grid with its perforated amorphous carbon film was pulled into contact with the substrate by evaporating a drop of solvent. Then, the grid along with the graphene sheet was floated off using a second drop of solvent. The as-prepared membranes were irradiated briefly in a conventional TEM or scanning electron microscope along the edges of the thin regions, thereby pinning them down by hydrocarbon deposits[12] (without this step, we found that the sheets may detach from the support and collapse into a crumpled configuration upon heating). Then, they were heated on a hot plate in air at 200 °C for 10 min, in order to reduce the amount of adsorbates, just prior to insertion into the high-resolution TEM.

* To whom correspondence should be addressed. E-mail: azettl@berkeley.edu.

† Materials Sciences Division, Lawrence Berkeley National Laboratory and Department of Physics, University of California at Berkeley.

‡ National Center for Electron Microscopy, Lawrence Berkeley National Laboratory.

10.1021/nl801386m CCC: $40.75 © XXXX American Chemical Society
Published on Web 06/19/2008

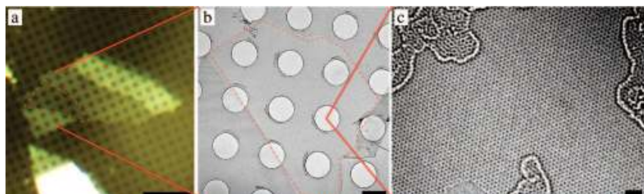

Figure 1. (a) Optical micrograph, and (b) low-magnification TEM image of graphene sheets on the perforated carbon film. A single-layer region is outlined by a red dashed line. (c) Unfiltered CCD exposure (1 s) of a single-layer graphene membrane. The structures near the edge of the image are adsorbates, and a hole (formed after prolonged irradiation) is seen near the lower-edge left. Scale bars are 10 μm (a), 1 μm (b), and 1 nm (c).

The high-resolution TEAM 0.5 microscope was operated at 80 kV with the third-order spherical aberration tuned to Cs $=-17$ μm. For a Schottky field-emission microscope, the resolution and the information limit at this operating voltage are limited by chromatic aberration. In order to achieve subangstrom resolution and information transfer, it is necessary to decrease the energy spread of the incoming electron beam. We therefore employed the gun electron monochromator in order to have an energy spread of 0.22 eV on the sample. Using a negative value of the third-order spherical aberration in combination with a positive fifth-order spherical aberration constant (5 mm), a small positive defocus yields white-atom contrast.[13–15] The images shown here were obtained for an overfocus of about 8 nm. At these settings, images can be interpreted directly in terms of the structure because the sample is small enough to be completely within the optimum focus window of about 1 nm.

Figure 1a shows an optical micrograph of a large graphene sample on the support grid (the 1-μm grid perforation holes are barely visible), whereas Figure 1b shows a low-magnification TEM image with the essentially invisible (at this magnification) single-layer graphene membrane spanning several holes. Figure 1c shows high-resolution TEM data obtained by zooming in on one of the suspended membrane regions. This image represents a single, unfiltered CCD exposure, and the intensity profile (carbon atoms are here white) is a direct and striking representation of the carbon atomic structure in graphene. The additional structure near the upper-left, upper-right, and bottom-center regions of the figure are adsorbates. Importantly, significant areas shown in Figure 1c appear clean and structurally perfect.

The exceptional resolution afforded by such microscopy allows detailed examination of the atomic structure of graphene, in particular contrast profile, single versus multilayers, and defect configurations. We first briefly summarize the image processing parameters and determine the signal-to-noise for detection of individual carbon atoms in the graphene lattice. Images (Figures 2 and 3) were high-pass filtered with a smooth cut off near 20 Å in order to compensate the slightly uneven illumination intensity. The exposure time was 1 s with a pixel size of 0.24 Å. After Fourier-filtering (i.e., essentially subtracting the ideal lattice; not shown), the images of the clean areas could not be distinguished from an image of empty space. We then estimated the noise after smoothing these empty images to the actual resolution of 1 Å (by either a low-pass filter or Gaussian blur). The resulting noise level (standard deviation) is about 0.8% (ca. 2% before smoothing). Thus, an individual carbon atom with a contrast of about 6% is detected against the noise even in single exposures (Figures 1c and 3a−d). Even better signal-to-noise ratios could be obtained by averaging drift-compensated images if features clearly did not change between subsequent exposures (Figures 2 and 3e−k).

A direct image of a single-layer graphene sheet (average of 7 exposures) is shown in Figure 2a along with the contrast profile (Figure 2b). Image simulations for the contrast profile, where the atoms are well-approximated as weak phase objects, are straightforward and were carried out using *MacTempas*, the computer code in ref 16 and our own computer code (based on scattering factors in refs and 18) for comparison, with very similar simulation results. Interestingly, although the form of the pattern matches very well, the simulated contrast is a factor of 2 greater than the contrast observed experimentally. Figure 2c shows a comparison of data to the simulation with the simulated contrast precisely halved; the match is remarkably good. This kind of correction may be related to the well-known so-called "Stobbs factor"[19,20] for imaging of three-dimensional samples. Therefore, we establish a correction factor of 2 in contrast of lattice images from a crystalline single layer of carbon recorded at 80 kV on the CCD camera.

Because single-layer graphene is only half a unit cell in the *c* axis of graphite, it has a unique signature in the direct image (as well as in a diffraction pattern). Figure 2d and e shows the difference at the step from a single to a bilayer region. The AB stacked bilayer region (bottom half of the figures) shows a qualitatively different pattern than the single-layer area. However, care must be taken in using such images for identification because the single-layer region indeed appears like a bilayer (and vice versa) at a different defocus. Here, electron-diffraction analysis was used to verify the presence of a single layer or bilayer.[21–23] Figure 2f shows the Fourier transform of a larger image of the bilayer region. The outermost set of peaks corresponds to an information transfer of 1.06 Å. The bilayer image is chosen here to demonstrate this extraordinary transfer because the third ring of spots is almost zero in the single-layer structure. This is the highest reflection that is visible in these ultrathin, low-contrast samples and may not represent the ultimate limit of the microscope. The two innermost sets of hexagons correspond to 2.13 and 1.23 Å. It must be noted that although resolving the 2.13 Å reflection provides lattice images of graphene already in moderate resolution microscopes, the individual carbon atoms in graphene are resolved only if the second reflection at 1.23 Å is transferred.

The real-time atomic-scale observation of the formation and dynamics of defects in graphene at this resolution has heretofore been experimentally inaccessible. The TEAM instrument makes these studies possible. The formation and dynamics of defects in single-layer graphene was observed by recording a sequence of images at or near the optimum

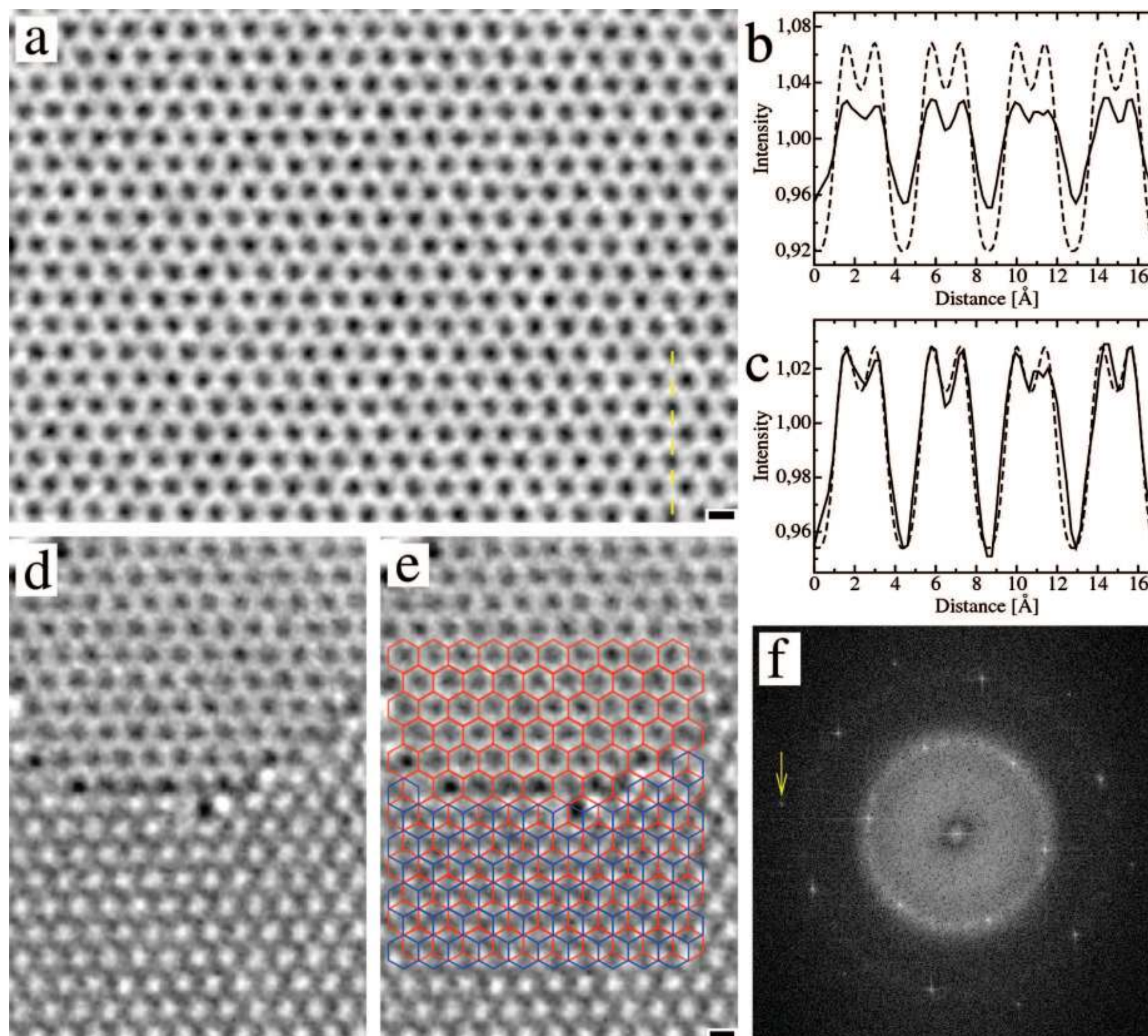

Figure 2. (a) Direct image of a single-layer graphene membrane (atoms appear white). (b) Contrast profile along the dotted line in panel a (solid) along with a simulated profile (dashed). The experimental contrast is a factor of 2 smaller: Panel c shows the same experimental profile with the simulated contrast scaled down by a factor of 2. (d and e) Step from a monolayer (upper part) to a bilayer (lower part of the image), showing the unique appearance of the monolayer. Panel e shows the same image with an overlay of the graphene lattice (red) and the second layer (blue), offset in the Bernal (AB) stacking of graphite. In the bilayer region, white dots appear where two carbon atoms align in the projection. (f) Numerical diffractogram, calculated from an image of the bilayer region. The outermost peaks, one of them indicated by the arrow, correspond to a resolution of 1.06 Å. The scale bars are 2 Å.

white-atom defocus parameter. Although the sample holder was maintained at room temperature, the observed region might have been heated by the electron beam. Figure 3 shows examples starting with the unperturbed lattice, the defect structure, and then again the ideal lattice after the defect has disappeared. An isolated Stone−Wales (SW) defect was found during one exposure (1 s) of the sequence and relaxed to the unperturbed lattice in the next exposure (4 s later) (Figure 3a−d). Defects consisting of multiple five- and seven-membered rings of carbon atoms spontaneously appeared and remained stable for up to 20 s. Remarkably, all defect configurations relax to the unperturbed graphene lattice and contain the same number of pentagons and heptagons in an arrangement that does not involve a dislocation or disclination. In addition, Figure 3e and f shows a reconstructed vacancy configuration involving a pentagon, which also returned to the unperturbed lattice after a few seconds. In this case, the missing carbon atom must have been replaced, from a mobile adsorbate, via surface diffusion on the graphene sheet.

Pentagon−heptagon (5−7) defects, in particular the Stone−Wales defect,[24] are proposed to play a key role in the formation and transformation of sp-2 bonded carbon nanostructures.[25] It is customarily assumed that, after formation of SW defects, pentagon−heptagon pairs separate, thereby inducing dislocations and curvature. These defects are involved in the coalescence of fullerenes and nanotubes,[25,26] and their mobility is relevant for the plastic response of carbon nanotubes under strain.[27] In our case of the (almost[22]) planar graphene membrane, however, the separation of pentagon−heptagon pairs is clearly not the favored pathway: In all cases we have observed, the multiple 5−7 defects relax to the original unperturbed lattice. This contrasts findings from highly curved graphene structures where the introduction of dislocations in the electron beam[9] and the motion of pentagons and heptagons[10] has been

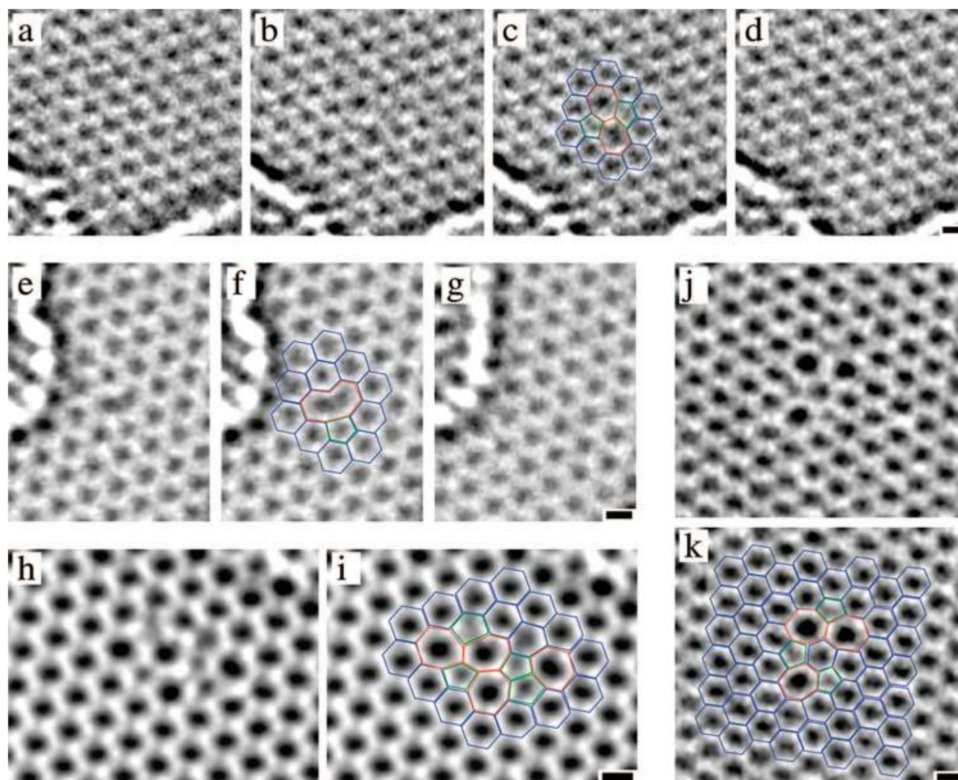

Figure 3. Metastable defects found in HRTEM image sequences. (a−d) Stone−Wales (SW) defect: (a) unperturbed lattice before appearance of the defect, (b) SW defect (c) same image with atomic configuration superimposed, (d) relaxation to unperturbed lattice (after ca. 4 s). (e−g) Reconstructed vacancy: (e) original image and (f) with atomic configuration; a pentagon is indicated in green. (g) Unperturbed lattice, 4 s later. (h and i) Defect image and configuration consisting of four pentagons (green) and heptagons (red). Note the two adjacent pentagons. (j and k) Defect image and configuration consisting of three pentagons (green) and three heptagons (red). This defect returned to the unperturbed lattice after 8 s. In spite of the odd number of 5−7 pairs, this is not a dislocation core (it is compensated by the rotated hexagon near the center of the structure). All scale bars are 2 Å.

observed. Evidently, the rearrangements after formation of a defect can transform a curved, closed-shell graphene derivative into a slightly different shape by local deformations (such as shrinking of single-walled carbon nanotubes in an electron beam[28]). However, in the planar geometry with a fixed boundary, this is not the case. This result also implies that the membranes are not under a significant strain that would favor the formation of dislocations. In a comparison experiment, we indeed found that graphene membranes are much more stable than single-walled carbon nanotubes under the same dose and voltage of the electron beam. The maximum energy that can be transferred from an 80 keV electron to a carbon atom is 15.6 eV, which is below the threshold for knock-on damage[29] but sufficient to form multiple SW defects.[24,27,26,25]

In conclusion, we have demonstrated direct imaging that resolves all individual carbon atoms in suspended single-layer graphene membranes. We find that the dynamics of defects in extended, two-dimensional graphene membranes are different than in closed-shell graphenes such as nanotubes or fullerenes. The study of defects, vacancies, and edges in graphene, as well as absorbates, is important for basic understanding of this novel material as well as for potential electronic, mechanical, and thermal applications. Low-voltage imaging in combination with aberration correction enables atomic resolution imaging of samples that are too fragile at higher electron energies, and the detection of individual carbon atoms is relevant for organic materials. Graphene membranes are highly promising as support structure for TEM imaging of other materials as well because the graphene provides a highly transparent, crystalline background, and the precisely known structure is an ideal tuning and calibration tool for electron microscopy developments.

Acknowledgment. NCEM is supported by the Department of Energy under contract no. DE-AC02-05CH11231. The TEAM project is supported by the Department of Energy, Office of Science, Office of Basic Energy Sciences. J.C.M., M.F., and A.Z. were supported by the Director, Office of Energy Research, Office of Basic Energy Sciences, Materials Sciences and Engineering Division, of the U.S. Department of Energy under contract no. DE-AC02-05CH11231, via the sp^2-bonded nanostructures program.

References

(1) Novoselov, K. S.; Geim, A. K.; Morozov, S. V.; Jiang, D.; Zhang, Y.; Dubonos, S. V.; Grigorieva, I. V.; Firsov, A. A. *Science* **2004**, *306*, 666.
(2) Novoselov, K. S.; Jiang, D.; Schedin, F.; Booth, T. J.; Khotkevich, V. V.; Morozov, S. V.; Geim, A. K. *Proc. Natl. Acad. Sci.* **2005**, *102*, 10451.
(3) Zhang, Y.; Tan, J. W.; Stormer, H. L.; Kim, P. *Nature* **2005**, *438*, 201.
(4) Novoselov, K. S.; Geim, A. K.; Morozov, S. V.; Jiang, D.; Katsnelson, M. I.; Grigorieva, L. V.; Dubonos, S. V.; Firsov, A. A. *Nature* **2005**, *438*, 197.

(5) Son, Y.-W.; Cohen, M. L.; Louie, S. G. *Nature* **2006**, *444*, 347.
(6) Heersche, H. B.; Jarillo-Herrero, P.; Oostinga, J. B.; Vandersypen, L. M. K.; Morpurgo, A. F. *Nature* **2007**, *446*, 56.
(7) http://ncem.lbl.gov/TEAM-project.
(8) Kisielowski, C.; Freitag, B.; Bischoff, M.; van Lin, H.; Lazar, S.; Knippels, G.; Tiemeijer, P.; van der Stam, M.; von Harrach, S.; Stekelenburg, M.; Haider, M.; Uhlemann, S.; Muller, H.; Hartel, P.; Kabius, B.; Miller, D.; Petrov, I.; Olson, E. A.; Donchev, T.; Kenik, E. A.; Lupini, A.; Bentley, J.; Pennycook, S.; Anderson, I. M.; Minor, A. M.; Schmid, A. K.; Duden, T.; Radmilovic, V.; Ramasse, Q.; Watanabe, M.; Erni, R.; Stach, E. A.; Denes, P.; Dahmen., U. *Nat. Mater.* **2008**, . in review.
(9) Hashimoto, A.; Suenaga, K.; Gloter, A.; Urita, K.; Iijima, S. *Nature* **2004**, *430*, 870.
(10) Suenaga, K.; Wakabayashi, H.; Koshino, M.; Sato, Y.; Urita, K.; Iijima, S. *Nat. Nanotechnol.* **2007**, *2*, 358.
(11) Smith, B. W.; Luzzi, E. *J. Appl. Phys.* **2001**, *90*, 3509.
(12) Meyer, J. C.; Girit, C. O.; Crommie, M. F.; Zettl, A. *Appl. Phys. Lett.* **2008**, *92*, 123110.
(13) Jia, C.-L.; Lentzen, M.; Urban, K. *Microsc. Microanal.* **2004**, *10*, 174.
(14) Lentzen, M.; Jahnen, B.; Jia, C. L.; Thust, A.; Tillmann, K.; Urban, K. *Ultramicroscopy* **2002**, *92*, 233.
(15) Jia, C. L.; Lentzen, M.; Urban, K. *Science* **2003**, *299*, 870.
(16) Kirkland. E. J. *Advanced Computing in Electron Microscopy*; Plenum Press: New York, 1998.
(17) Doyle, P. A.; Turner, P. S. *Acta Crystallogr., A* **1968**, *24*, 390.
(18) Peng, L.-M.; Ren, G.; Dudarev, S. L.; Whelan, M. J. *Acta Crystallogr., A* **1996**, *52*, 257.
(19) Hytch, M. J.; Stobbs, W. M. *Ultramicroscopy* **1994**, *53*, 191.
(20) Howie, A. *Ultramicroscopy* **2004**, *98*, 73.
(21) Ferrari, A. C.; Meyer, J. C.; Scardaci, V.; Casiraghi, C.; Lazzeri, M.; Mauri, F.; Piscanec, S.; Jiang, D.; Novoselov, K. S.; Roth, S.; Geim, A. K. *Phys. Rev. Lett.* **2006**, *97*, 187401.
(22) Meyer, J. C.; Geim, A. K.; Katsnelson, M. I.; Novoselov, K. S.; Booth, T. J.; Roth, S. *Nature* **2007**, *446*, 60.
(23) Meyer, J. C.; Geim, A. K.; Katsnelson, M. I.; Novoselov, K. S.; Obergfell, D.; Roth, S.; Girit, C.; Zettl, A. *Solid State Commun.* **2007**, *143*, 101.
(24) Stone, A. J.; Wales, D. J. *Chem. Phys. Lett.* **1986**, *128*, 501.
(25) Yoon, M.; Han, S.; Kim, G.; Lee, S. B.; Berber, S.; Osawa, E.; Ihm, J.; Terrones, M.; Banhart, F.; Charlier, J.-C.; Grobert, N.; Terrones, H.; Ajayan, P. M.; Tomanek, D. *Phys. Rev. Lett.* **2004**, *92*, 075504.
(26) Kim, Y.-H.; Lee, I.-H.; Chang, K. J.; Lee, S. *Phys. Rev. Lett.* **2003**, *90*, 065501.
(27) Nardelli, M. B.; Yakobson, B. I.; Bernholc, J. *Phys. Rev. Lett.* **1998**, *81*, 4656.
(28) Banhart, F. *Rep. Prog. Phys.* **1999**, *62*, 1181.
(29) Zobelli, A.; Gloter, A.; Ewels, C. P.; Seifert, G.; Colliex, C. *Phys. Rev. B* **2007**, *75*, 245402.

NL801386M